Circulation
JOURNAL OF THE AMERICAN HEART ASSOCIATION

American Heart Association®

Mineralocorticoid Modulation of Cardiac Ryanodine Receptor Activity Is Associated With Downregulation of FK506-Binding Proteins

Ana María Gómez, Angélica Rueda, Yannis Sainte-Marie, Laetitia Pereira, Spyros Zissimopoulos, Xinsheng Zhu, Roxane Schaub, Emeline Perrier, Romain Perrier, Céline Latouche, Sylvain Richard, Marie-Christine Picot, Frederic Jaisser, F. Anthony Lai, Héctor H. Valdivia and Jean-Pierre Benitah

Circulation. 2009;119:2179-2187; originally published online April 13, 2009;
doi: 10.1161/CIRCULATIONAHA.108.805804
Circulation is published by the American Heart Association, 7272 Greenville Avenue, Dallas, TX 75231
Copyright © 2009 American Heart Association, Inc. All rights reserved.
Print ISSN: 0009-7322. Online ISSN: 1524-4539

The online version of this article, along with updated information and services, is located on the World Wide Web at:
http://circ.ahajournals.org/content/119/16/2179

Data Supplement (unedited) at:
http://circ.ahajournals.org/content/suppl/2009/04/24/CIRCULATIONAHA.108.805804.DC1.html

Permissions: Requests for permissions to reproduce figures, tables, or portions of articles originally published in *Circulation* can be obtained via RightsLink, a service of the Copyright Clearance Center, not the Editorial Office. Once the online version of the published article for which permission is being requested is located, click Request Permissions in the middle column of the Web page under Services. Further information about this process is available in the Permissions and Rights Question and Answer document.

Reprints: Information about reprints can be found online at:
http://www.lww.com/reprints

Subscriptions: Information about subscribing to *Circulation* is online at:
http://circ.ahajournals.org//subscriptions/

Downloaded from http://circ.ahajournals.org/ at Cardiff University on February 19, 2014

Mineralocorticoid Modulation of Cardiac Ryanodine Receptor Activity Is Associated With Downregulation of FK506-Binding Proteins

Ana María Gómez, PhD; Angélica Rueda, PhD; Yannis Sainte-Marie, PhD; Laetitia Pereira, PhD; Spyros Zissimopoulos, PhD; Xinsheng Zhu, PhD; Roxane Schaub, MD; Emeline Perrier, PhD; Romain Perrier, PhD; Céline Latouche, MS; Sylvain Richard, PhD; Marie-Christine Picot, MD, PhD; Frederic Jaisser, MD, PhD; F. Anthony Lai, PhD; Héctor H. Valdivia, MD, PhD; Jean-Pierre Benitah, PhD

Background—The mineralocorticoid pathway is involved in cardiac arrhythmias associated with heart failure through mechanisms that are incompletely understood. Defective regulation of the cardiac ryanodine receptor (RyR) is an important cause of the initiation of arrhythmias. Here, we examined whether the aldosterone pathway might modulate RyR function.

Methods and Results—Using the whole-cell patch clamp method, we observed an increase in the occurrence of delayed afterdepolarizations during action potential recordings in isolated adult rat ventricular myocytes exposed for 48 hours to aldosterone 100 nmol/L, in freshly isolated myocytes from transgenic mice with human mineralocorticoid receptor expression in the heart, and in wild-type littermates treated with aldosterone. Sarcoplasmic reticulum Ca^{2+} load and RyR expression were not altered; however, RyR activity, visualized in situ by confocal microscopy, was increased in all cells, as evidenced by an increased occurrence and redistribution to long-lasting and broader populations of spontaneous Ca^{2+} sparks. These changes were associated with downregulation of FK506-binding proteins (FKBP12 and 12.6), regulatory proteins of the RyR macromolecular complex.

Conclusions—We suggest that in addition to modulation of Ca^{2+} influx, overstimulation of the cardiac mineralocorticoid pathway in the heart might be a major upstream factor for aberrant Ca^{2+} release during diastole, which contributes to cardiac arrhythmia in heart failure. **(*Circulation*. 2009;119:2179-2187.)**

Key Words: aldosterone ■ calcium ■ ryanodine receptor ■ hormones ■ ion channels ■ arrhythmia

During the past decade, research has focused on the actions of aldosterone in target organs beyond the kidney, expanding the role of the aldosterone pathway in cardiovascular pathogenesis.[1] Indeed, mineralocorticoid receptors (MRs), which mainly underlie aldosterone action, have been detected in a range of nonrenal tissues, including the brain, blood vessels, and heart,[2] which suggests a broader pattern of biological activity for aldosterone than previously anticipated. The pivotal role of aldosterone, causing sodium retention with expansion of the extracellular volume that results in deterioration of hemodynamic responsiveness and a fall in cardiac output, has long been recognized in heart failure (HF).[3,4] In addition, accumulating experimental and clinical evidence suggests that aldosterone has direct adverse cardiac effects independent of its effects on blood pressure, especially an increased risk of arrhythmic death.[3,4] Interestingly, major clinical trials involving MR antagonists have shown significant benefits on risk of cardiovascular events, in particular sudden death in HF.[5,6] A pertinent question, therefore, is how activation of cardiac MR participates in life-threatening arrhythmias.

Clinical Perspective p 2187

Most fatal arrhythmias in experimental HF are initiated by nonreentrant mechanisms that arise from abnormal ventricular automaticity or triggered activity.[7,8] The latter consists of either early afterdepolarizations (EADs) that occur in the plateau phase of the action potential (AP) or delayed afterdepolarizations (DADs) that occur at repolarized membrane potentials.[9] EADs typically occur in the setting of prolonged repolarization due to

Received July 16, 2007; accepted March 3, 2009.

From INSERM, U637 (A.M.G., A.R., L.P., E.P., R.P., S.R., J.-P.B.), Université Montpellier, France; INSERM, U772 (Y.S.-M., C.L., F.J.), Collège de France, Paris, France; Wales Heart Research Institute (S.Z., F.A.L.), Cardiff University School of Medicine, Cardiff, United Kingdom; Department of Physiology (X.Z., H.H.V.), University of Wisconsin Medical School, Madison, Wis; and Département de l'Information Médicale (R.S., M.-C.P.), Hôpital Lapeyronie, CHU Montpellier, France.

The online-only Data Supplement is available with this article at http://circ.ahajournals.org/cgi/content/full/CIRCULATIONAHA.108.805804/DC1.

Correspondence to Jean-Pierre Benitah, Laboratoire de physiopathologie cardiovasculaire, INSERM U637, CHU Arnaud de Villeneuve, 34295 Montpellier, France. E-mail jean-pierre.benitah@inserm.fr

© 2009 American Heart Association, Inc.

Circulation **is available at http://circ.ahajournals.org** **DOI: 10.1161/CIRCULATIONAHA.108.805804**

Downloaded from http://circ.ahajournals.org/ at Cardiff University on February 19, 2014

alterations in ionic currents and to reactivation of the Ca^{2+} current (I_{Ca}). DADs are caused by membrane depolarization initiated by spontaneous Ca^{2+} release from the sarcoplasmic reticulum (SR) through the ryanodine receptor (RyR). We have accumulated evidence, both ex vivo and in vivo, that modulation of Ca^{2+} influx is a central factor in the cardiac action of the aldosterone pathway[10–14] and might be involved in EAD-related fatal ventricular tachyarrhythmia.[14] Moreover, enhanced diastolic leak of Ca^{2+} via RyRs generates DADs and is a fundamental mechanism underlying several genetic or acquired arrhythmias.[15,16] Therefore, we tested whether activation of the aldosterone pathway modulates diastolic RyR activity in heart.

Methods

All experiments were performed according to European Union Council Directives (86/609/EEC) for the care of laboratory animals. A detailed Methods section can be found in the online-only Data Supplement.

Cell Isolation and Incubation

Isolated ventricular myocytes from adult male Wistar rats (250 to 350 g; Elevage Janvier, Le Genest Saint Isle, France) were incubated for 48 hours, with or without D-aldosterone 100 nmol/L (Sigma, Saint Quentin Fallaviere, France). In some experiments, RU28318 10 μmol/L was added to aldosterone.[10,11]

Human MR Transgenic Mice and In Vivo Aldosterone Exposure

Cardiac-specific expression of human MR (hMR) was obtained by crossing a tetO-hMR mouse strain with an α-MHC-tTA transactivator mouse strain.[14] Littermate wild-type, gender-matched mice (WT) were used as controls. In some of these, after pentobarbital sodium anesthesia (30 mg/kg) was administered, osmotic minipumps (model 2 ML4, Alza Corp, Mountain View, Calif) were implanted subcutaneously for constant delivery of D-aldosterone 50 μg/d (dissolved in 0.9% saline) over 3 weeks. Chronic aldosterone infusion significantly increased the plasma aldosterone concentration above control levels (from 278±77 [n=7] to 1374±150 [n=7] pg/mL, $P<0.05$). Mice were devoid of cardiac hypertrophy either on the whole-organ level (heart weight–to–body weight ratio 5.9±0.4 [n=15], 5.9±0.3 [n=11], and 5.3±0.4 mg/g [n=6] in WT, aldosterone-treated, and hMR mice, respectively; $P>0.05$) or at the cellular level (membrane capacitance 201.8±6.1 [n=30], 199.6±12.7 [n=21], and 199.0±11.0 pF [n=26] for isolated ventricular myocytes from WT, aldosterone-treated, and hMR mice, respectively; $P>0.05$).

AP Recording

The whole-cell patch-clamp method was used in the current-clamp configuration to record APs with solutions and protocol as described previously.[11]

Spontaneous Local SR Ca^{2+} Release: Ca^{2+} Sparks

Fluo-3AM–loaded cells were imaged in Tyrode solution (in mmol/L: NaCl 130, NaH_2PO_4 0.4, $NaHCO_3$ 5.8, $CaCl_2$ 1, $MgCl_2$ 0.5, KCl 5.4, glucose 22, HEPES 25, insulin 0.01, pH 7.4) with a confocal microscope in line-scan mode.[11]

Cell Lysate and SR-Enriched Membrane Fraction (SR Fraction)

Cell lysates were prepared with homogenization buffer (in mmol/L: sucrose 300, NaF 20, HEPES 20, aprotinin 5.2 10^{-4}, benzamidine 0.5, leupeptin, 0.012, PMSF 0.1, pH 7.2) with a Potter-Elvehjem homogenizer and spun at 2000 *g* for 10 minutes. SR fractions were isolated by ultracentrifugation at 40 000 *g* for 30 minutes at 4°C.[17] Protein concentration by the Bradford method and binding of [^{3}H]ryanodine to SR fractions were assessed.[17]

Single-Channel Recordings

Analysis of RyR single-channel activity was done by fusing SR vesicles into planar lipid bilayers with Cs^+ as a charge carrier.[17] Only bilayers that contained a single channel were used. Channel activity was always tested for sensitivity to EGTA, which was added in the cis chamber at the end of each experiment.

Reverse-Transcription Polymerase Chain Reaction Analysis

Total RNA was extracted with Trizol (Invitrogen, Cergy Pontoise, France). First-strand cDNA was synthesized after DNaseI treatment (DNAfree, Ambion, Courtaboeuf, France) with 1 μg of total RNA, random hexamers (Amersham, Biosciences Europe GMBH, Orsay, France), and Superscript II reverse transcriptase (Invitrogen). Transcript levels were analyzed in triplicate by real-time polymerase chain reaction with an iCycler iQ apparatus (Bio-Rad, Marnes la Coquette, France) with a qPCR Core Kit for SYBR Green I (Eurogentec, Brussels, Belgium) that contained 500 nmol/L of specific primers (Data Supplement, Table I) and 3 μL of diluted template cDNA. Relative expression of FK506-binding proteins (FKBPs) and RyR was normalized by the geometric average of relative quantities for reference genes. Serial dilutions of pooled cDNA were used in each experiment to assess the efficiency of the polymerase chain reaction.

Immunoblots

Immunoblots were prepared from cell lysates with anti-FKBP12/12.6 (1:1000, Santa-Cruz Biotechnology Inc, Santa Cruz, Calif), anti-RyR (1:3000, Affinity BioReagents, Golden, Colo), and anti-actin (1:20 000, Sigma) antibodies. FKBP12/12.6-RyR interaction was assessed on SR fractions with anti-FKBP12/12.6 (1:200) and anti-RyR (1:1000) antibodies from Affinity BioReagents. Immunoblots of RyR phosphorylation were performed with anti–RyR-PS2809 (1:5000) antibody from Badrilla (Leeds, West Yorkshire, United Kingdom) and anti–RyR-PS2815 (1:5000) antibody generously provided by Dr A.R. Marks (Columbia University, New York, NY).

Statistical Analysis

Preliminary descriptive analyses include frequencies for categorical variables and mean±SD for continuous variables. A conditional hierarchical linear model was used (SAS/UNIX statistical software, SAS Institute, Cary, NC; proc mixed) to compare continuous variables between groups to take into account the multiple observations per animal. The group was a fixed effect, and animals were a random effect nested in the group; in the case of repeated measurements on cells, we add a random effect for cell in animal.

Data are presented as mean±SEM and were compared with Student's *t* test (for 2 groups) or ANOVA (for >2 groups, followed by a post hoc pairwise Tukey's honestly significant difference test). Significance was defined at $P<0.05$.

The authors had full access to and take full responsibility for the integrity of the data. All authors have read and agree to the manuscript as written.

Results

Aldosterone Pathway Increases Occurrence of DADs

During AP recordings, at 0.1-Hz cycle length in ventricular myocytes isolated from transgenic mice expressing hMR in the heart (hMR mice; Figure 1A), we observed oscillations in membrane potential after completion of the driven AP (Figure 1A, middle). Eventually, the DAD was large enough to reach the threshold to trigger spontaneous AP (Figure 1A, right). The occurrence of DADs was greatly enhanced by activation of the aldosterone pathway (Figure 1B). Ex vivo, after 48 hours' exposure of isolated rat ventricular myocytes to aldosterone 100 nmol/L, the occurrence of DADs increased compared with

Downloaded from http://circ.ahajournals.org/ at Cardiff University on February 19, 2014

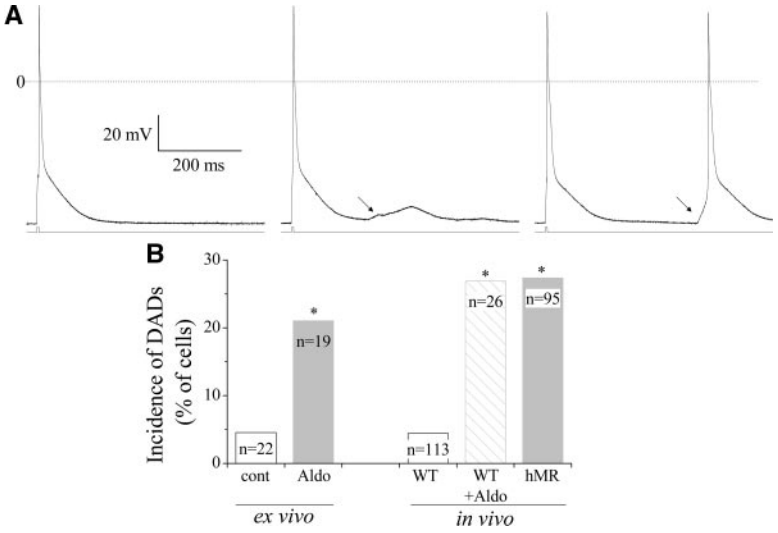

Figure 1. Activation of aldosterone pathway increases occurrence of DADs. A, Representative APs recorded from the same hMR cardiomyocyte, elicited at 0.1 Hz, showing the appearance of spontaneous depolarization (middle; DAD indicated by arrow) and triggering spontaneous AP (right). B, Bar graph plots number of cells presenting at least 1 DAD in rat ventricular myocytes incubated 48 hours with or without aldosterone 100 nmol/L and in ventricular myocytes isolated from WT, aldosterone-treated WT, and hMR littermate mice. n Indicates total cell number. *$P<0.05$. Aldo indicates aldosterone; cont, control.

control myocytes kept 48 hours in the absence of aldosterone. Likewise, in vivo, increases of DAD occurrence appeared after 3-week minipump infusion of aldosterone in WT mice or in hMR mice compared with untreated WT littermates.

Modulation of Ca^{2+} Sparks by Aldosterone Pathway

DADs are commonly initiated by nonelectrically driven, spontaneous Ca^{2+} release from the SR via the RyRs.[8] We thus examined the properties of RyRs in situ by visualizing spontaneous Ca^{2+} sparks, which reflect brief and local Ca^{2+} release events that occur when RyRs open.[18,19] Figure 2A shows line-scan images of cells isolated from WT, aldosterone-treated, and hMR mice. Either elevated circulating aldosterone or cardiac hMR expression resulted in an ≈1.6-fold increase of Ca^{2+} spark frequency (supplemental Table II; Figure 2B). No differences in mean values for Ca^{2+} spark amplitude (Figure 2C) or rise time (Figure 2D) were seen among the 3 groups. As seen in Figure 2A, in addition to classic Ca^{2+} sparks characterized by a brief, localized increase in the fluorescence signal (a half-time of decay of ≈30 ms and a diameter of ≈2 μm),[18] we also observed the appearance of widened (>4 μm) and long-lasting Ca^{2+}

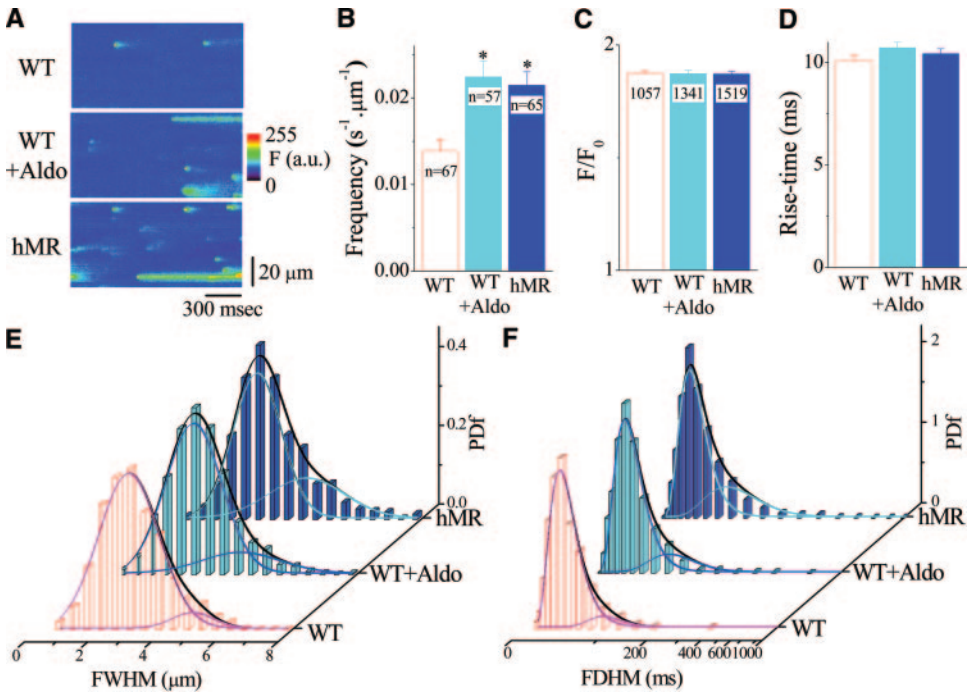

Figure 2. Change of spatiotemporal properties of Ca^{2+} sparks induced by mineralocorticoid in vivo. A, Sample line-scan fluorescence images record from cells isolated from WT (top), aldosterone-treated (WT+Aldo; middle), and hMR (bottom) mice. B through D, Comparison of frequency of occurrence, amplitude (F/F_0), and rise time of Ca^{2+} sparks at rest in myocytes from WT (open bars), WT+Aldo, (light blue bars), and hMR (blue bars) mice. In B, n is the cell number, whereas in C and D, it is the number of Ca^{2+} sparks. *$P<0.05$. Probability density function (PDf) of Ca^{2+} spark widths (E; FWHM) and durations (F; FDHM) at half-maximal amplitude in WT, WT+Aldo, and hMR mice. Curves represent mixed gaussian functions fitted to the histograms. In F, analyses were conducted on log(FDHM), and corresponding results are presented after back transformation.

Downloaded from http://circ.ahajournals.org/ at Cardiff University on February 19, 2014

Table. Mean (μ), SD (σ), Proportion (p, in %), and Coefficient of Determination (r^2) of Gaussian Fits to Ca^{2+} Spark Parameters

	FWHM, μm							FDHM, ms						
	μ_1	σ_1	p_1	μ_2	σ_2	p_2	r^2	μ_1	σ_1	p_1	μ_2	σ_2	p_2	r^2
Aldo in vivo														
WT	2.79	0.91	93.5	4.32	0.60	6.5	0.98	30.9	5.6	96.0	85.2	23.9	4.0	0.98
WT+Aldo	2.80	0.84	83.8	4.30	1.20	16.2	0.99	32.4	5.9	91.0	87.6	30.2	9.0	0.99
hMR	2.78	0.71	70.2	4.33	1.15	28.8	0.99	33.4	5.9	81.6	89.4	27.9	18.4	0.99
Aldo ex vivo														
Control	2.61	0.89	94.5	4.85	0.71	5.5	0.99	33.7	6.3	94.0	103.0	41.1	6.0	0.99
Aldo	2.62	0.91	72.0	4.60	1.25	28.0	0.99	33.5	6.3	81.7	106.0	50.3	18.3	0.99
Aldo+RU	2.54	0.78	95.8	4.53	0.70	4.2	0.99	33.7	5.7	95.7	105.3	35.2	4.3	0.99

Aldo indicates aldosterone; FWHM and FDHM, full width and duration at half-maximal amplitude; and Aldo+RU, aldosterone plus RU28318 (10 μmol/L).

release events (>80 ms). A mixed-effects model revealed increases of both averaged Ca^{2+} spark full widths and full durations at half-maximal amplitude in aldosterone-treated and hMR mice (supplemental Table II), which might reflect differences in population proportions. The distributions of full width and full duration at half maximum were empirically fitted to bimodal gaussian functions (Figure 2E and 2F). The distributions of full width at half maximum showed a prominent mode near 2.8 μm and a second minor mode near 4.3 μm, regardless of the conditions; however, the proportion of events that showed a larger width was greater in aldosterone-treated and hMR mice than in WT mice (Table). Moreover, events that lasted >50 ms were more frequent in aldosterone-treated and hMR mice than in WT mice. Distributions of log(full duration at half maximum) were fitted by 2 gaussian distributions with 2 distinct peaks at ≈32 and 87 ms, but the frequencies of long-lasting signals were greater in aldosterone-treated and hMR mice than in WT mice (Table). No correlation between Ca^{2+} spark spatiotemporal characteristics was observed. This is consistent with the occurrence of 3 different populations of Ca^{2+} sparks, the redistribution of which to long-lasting and more widespread populations was increased by activation of the cardiac aldosterone pathway.

Although the effects of aldosterone in vivo are presumably due to its direct cardiomyocyte effect, aldosterone might cause release of second messengers from noncardiac cells that can affect Ca^{2+} sparks. To exclude this possibility, we examined the properties of spontaneous Ca^{2+} sparks of isolated rat ventricular

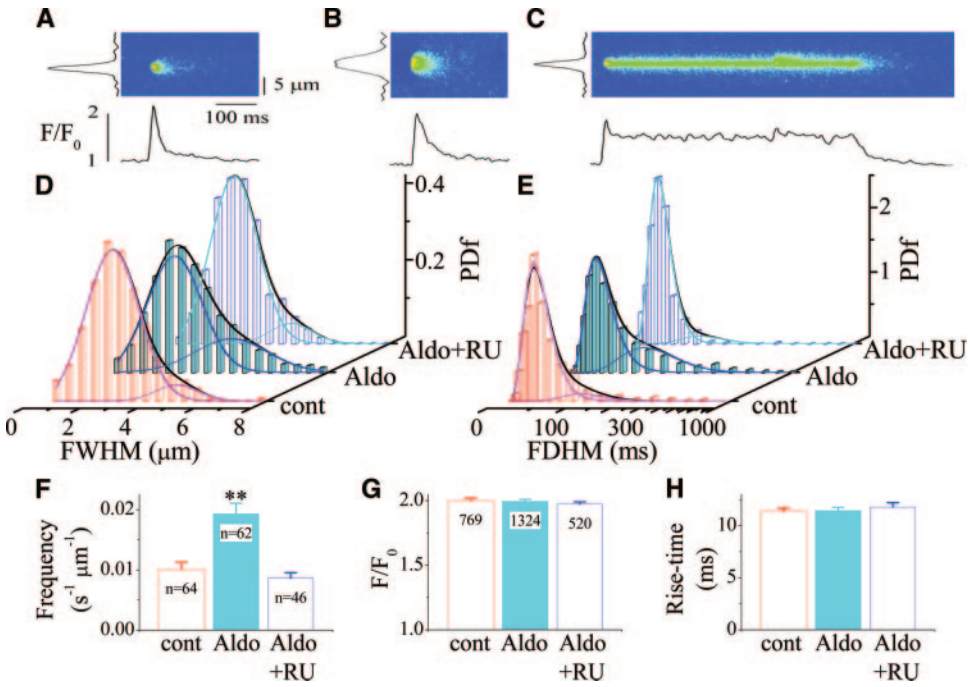

Figure 3. Ex vivo aldosterone exposure promotes the occurrence of widespread and long-lasting Ca^{2+} sparks. A through C, Representative spark images and spatiotemporal profiles from a 48-hour aldosterone-treated cell showing that spontaneous Ca^{2+} sparks can be short (A), large (B), or long (C). The distance along the cell is represented vertically, and the time is represented horizontally. D and E, Probability density function (PDf) of full width (FWHM) and full duration (FDHM) at half-maximal amplitude after 48 hours' incubation under conditions of control (cont; red open bars) and 100-nmol/L aldosterone without (Aldo; blue bars) and with (Aldo+RU; blue open bars) 10-μmol/L RU28318. Histograms were fitted by the sum of 2 gaussian distributions. F through H, Bar graphs of mean±SEM values for Ca^{2+} spark frequency (F), amplitude (F/F_0; G), and rise time (H). In F, n is the cell number, whereas in G and H, it is the number of Ca^{2+} sparks. $^{**}P<0.005$.

Downloaded from http://circ.ahajournals.org/ at Cardiff University on February 19, 2014

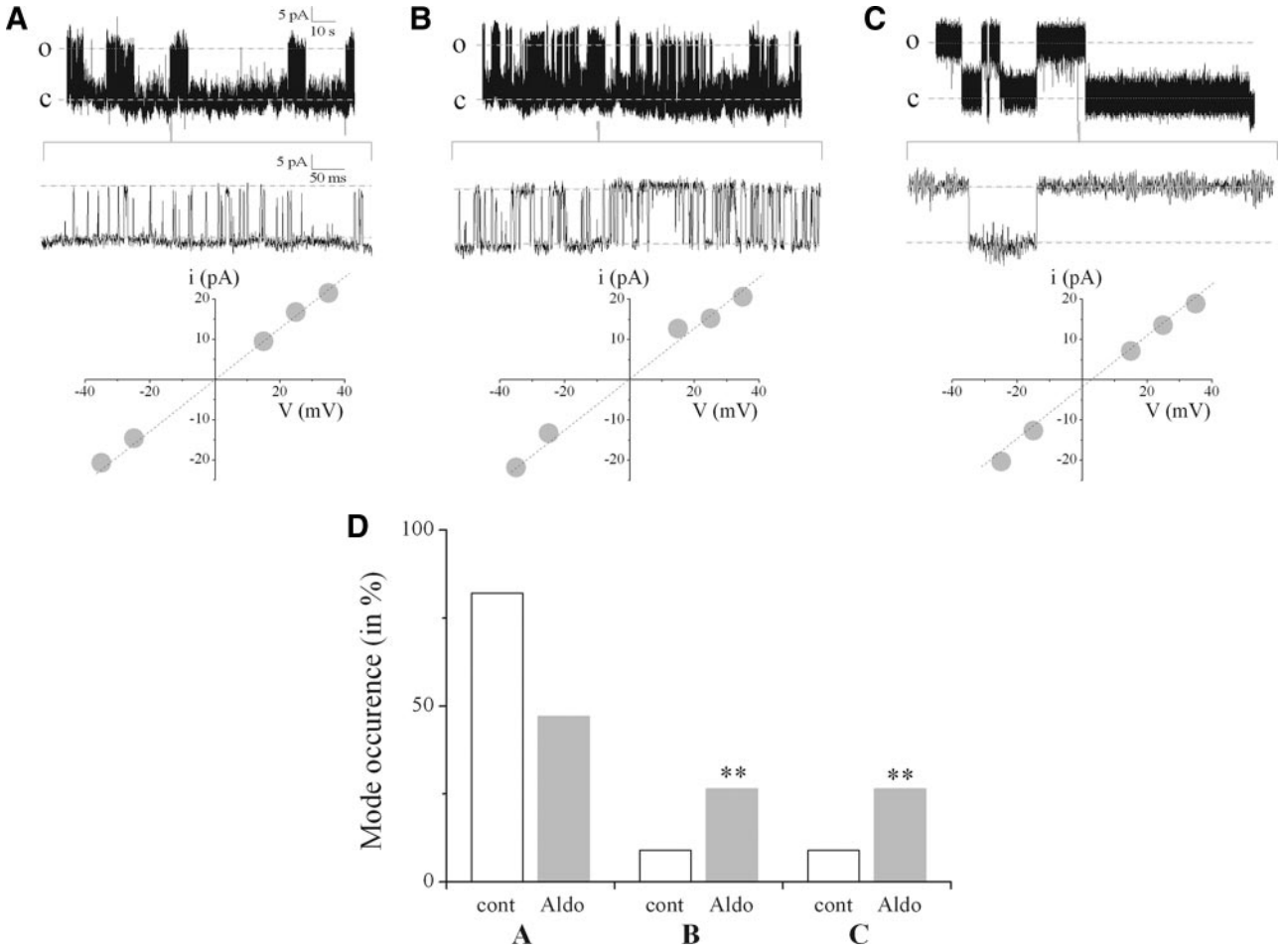

Figure 4. Single RyR channels reconstituted in lipid bilayers display 3 different kinetic behaviors: (A) Short, (B) burst, and (C) long openings. Each panel shows representative examples of single-channel behaviors of RyR reconstituted from the same SR-enriched membrane fraction of rat ventricular myocytes incubated 48 hours in the presence of aldosterone. Top, 2-minute and 500-ms section of the recording on an expanded time scale of single-channel traces recorded at 25 mV with channel openings (o) in the upward direction; Bottom, current-voltage relationship of the corresponding incorporated RyR. D, Bar graph plots the percentage of the occurrence of modal behaviors of reconstituted RyR channels from SR fractions of cells kept 48 hours with (Aldo, shaded bars, n=15) and without aldosterone (cont, open bars, n=11). $^{**}P<0.005$.

myocytes kept 48 hours with or without aldosterone 100 nmol/L. Three different populations of Ca^{2+} sparks were observed (Figure 3): The normal Ca^{2+} sparks were narrow and brief (Figure 3A); the second population was substantially wider in space but only slightly longer in duration (Figure 3B); and the third population had the same width as the normal population but was much longer in duration (Figure 3C). Analysis of the distributions of full width at half maximum (Figure 3D) and full duration at half maximum (Figure 3E) showed that ex vivo aldosterone exposure increased the occurrence of both wider and longer populations (Table; supplemental Table II). In addition, we observed a 1.9-fold increase in Ca^{2+} spark frequency (supplemental Table II; Figure 3F), whereas mean Ca^{2+} spark amplitude (Figure 3G) and rise time (Figure 3H) were not affected. Coincubation with a specific MR antagonist, RU28318,[11–13] prevented aldosterone-induced changes in Ca^{2+} spark properties (Figure 3).

Aldosterone Effects on Ca^{2+} Sparks Might Arise From Modulation of RyR Intrinsic Properties

The open probability of RyRs is influenced by the amount of Ca^{2+} stored in the SR.[20] A potential increase of SR Ca^{2+} load by aldosterone could therefore underlie the observed effects on Ca^{2+} sparks. SR Ca^{2+} load was estimated by rapid caffeine application (10 mmol/L) in the same intact cells used for Ca^{2+} sparks.[11,21] No difference ($P>0.05$) was observed in hMR mice (peak ratio of fluorescence intensity [F/F_0] 4.0±0.1, n=56) or aldosterone-treated mice (3.8±0.2, n=43) compared with WT mice (4.1±0.1, n=29). In addition, no difference in caffeine-evoked Ca^{2+} transients was noted after ex vivo aldosterone exposure (3.7±0.2 and 4.0±0.2 in control [n=13] and aldosterone-treated [n=13] myocytes, respectively; $P>0.05$). These results are consistent with the absence of alteration in Ca^{2+} spark amplitude and suggest that aldosterone does not modulate RyR activity (and hence, Ca^{2+} sparks) by altering SR content.

Ca^{2+} sparks result from the opening of clusters of RyRs; thus, increased Ca^{2+} spark frequency might result from increased RyR expression. Immunoblot analysis of cell lysates showed similar RyR amounts; after normalization against control, ratios of RyR to actin levels were 1±0.3 (n=8), 0.95±0.3 (n=4), and 0.82±0.3 (n=4) in WT, WT plus aldosterone, and hMR mice, respectively ($P>0.05$) and 1±0.2 (n=8) and 0.94±0.2 (n=4) in rat ventricular myocytes kept 48 hours without and with aldo-

Downloaded from http://circ.ahajournals.org/ at Cardiff University on February 19, 2014

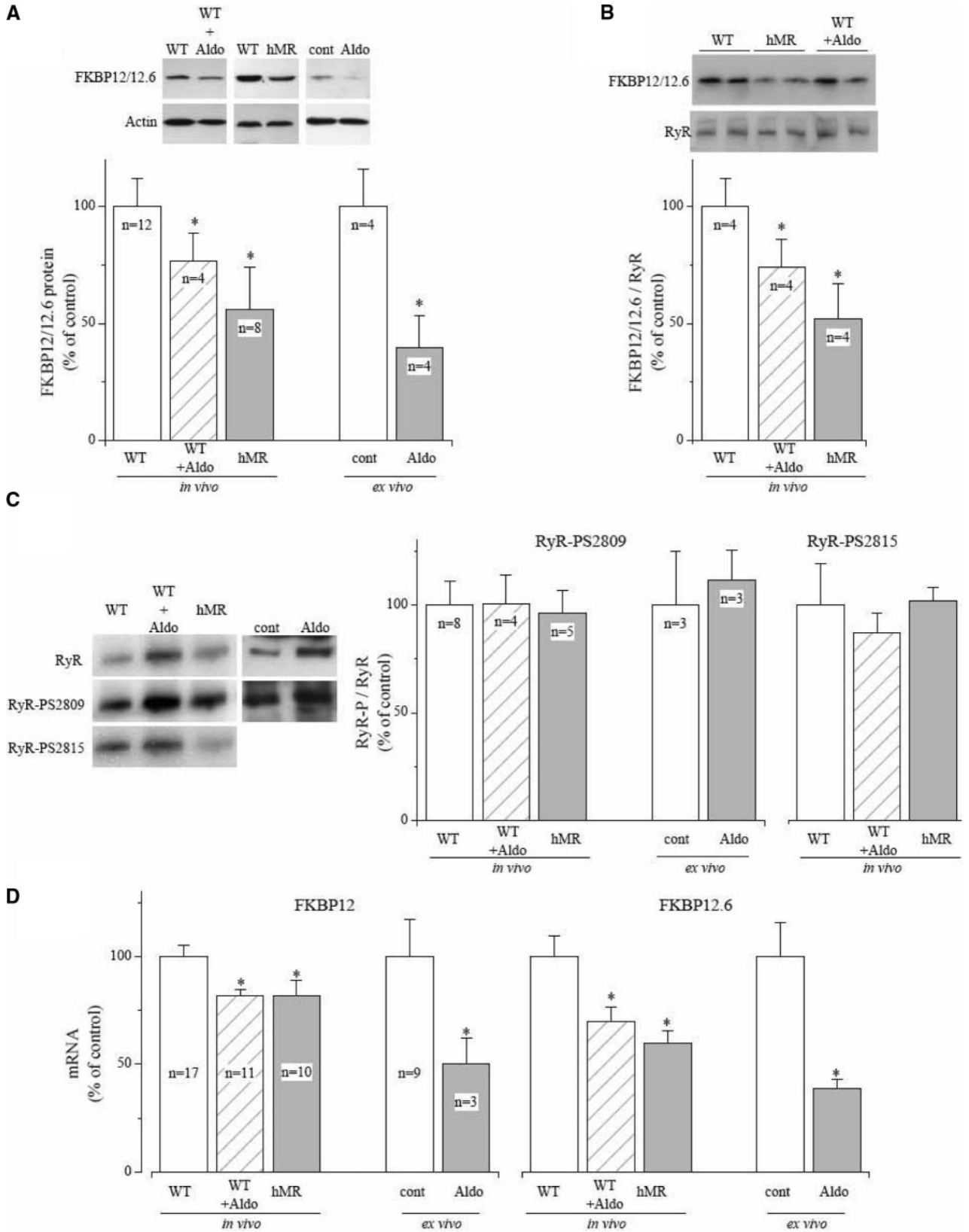

Figure 5. Downregulation of FKBP12 and FKBP12.6 expression after activation of cardiac aldosterone pathway. A–C, Representative immunoblots and quantification of (A) FKBP12/12.6 protein levels in cardiac cell lysates (normalized to the corresponding actin level and to respective controls) and (B) FKBP12/12.6 and RyR content in SR-enriched membrane fractions (cumulative data presented are derived from 4 different heart preparations, each immunoblotted 4 times, and are illustrated after normalization against the WT, non-treated sample). C, Pooled data represent ratios of RyR-P2815 and RyR-P2809 to RyR from SR-enriched membrane fractions normalized

(*Continued*)

Downloaded from http://circ.ahajournals.org/ at Cardiff University on February 19, 2014

sterone, respectively ($P>0.05$). RyR expression of isolated rat cardiomyocytes kept 48 hours with or without aldosterone, examined by [^{3}H]ryanodine binding to SR fractions, indicated unchanged high-affinity binding site for ryanodine (K_d values in nmol/L: 1.5±0.2 and 1.8±0.4 after 48 hours' incubation with [n=6] and without aldosterone [n=6], respectively; $P>0.05$) and similar expression levels of RyR after aldosterone exposure (maximal receptor density 0.24±0.04 and 0.29±0.03 pmol/mg protein, respectively; $P>0.05$).

These results show that activation of the aldosterone pathway in cardiac myocytes altered Ca^{2+} spark properties without modifying SR Ca^{2+} content or RyR expression. Therefore, aldosterone modulation of Ca^{2+} sparks might arise from changes in the intrinsic activity of the RyR complex. As an index, we fused SR fractions from control and aldosterone-treated rat cardiomyocytes into planar lipid bilayers to record single-channel activity of RyR. In addition to classic bimodal gating,[20] characterized by sequences of flickering openings with low (Figure 4A) and high (Figure 4B) open probability, clearly distinct, long, relatively stable openings with similar unitary current amplitude were observed (Figure 4C). Measurements from holding potentials from −35 to 35 mV showed that current-voltage relationships had similar conductances of 639, 632, and 640 pS (Figures 4A, 4B, and 4C, respectively). These results suggest that all recorded channel activity corresponded to RyRs; however, although the burst and long-lasting modes were observed in channels with and without aldosterone treatment, these modes occurred more frequently after aldosterone exposure (Figure 4D).

FKBP12/12.6 Downregulation by Mineralocorticoid Pathway

Taken together, the present results indicate that aldosterone through MR increases the likelihood that RyRs will open abnormally during diastole, which might reflect changes in intrinsic properties of the RyR. Activity of RyRs is tightly regulated by several accessory proteins that form a macromolecular signaling complex with RyR.[15,16] Among these ancillary proteins, FKBP12 and FKBP12.6 have been involved in the incidence of subsets of cardiac Ca^{2+} sparks with longer duration and wider spatial spread, along with increased frequency.[21–23] Therefore, we assessed the expression of FKBP12/12.6 protein levels. Compared with the respective controls, immunoblot analysis of cell lysates showed decreases in the amount of FKBP12/12.6 relative to actin levels after in vivo or ex vivo aldosterone exposure and in hMR mice (Figure 5A). The RyR-FKBP12/12.6 association was assessed indirectly by measurement of the ratio of FKBP12/12.6 to RyR detected in the SR fractions.[24–26] Immunoblot analysis indicated that the relative amount of FKBP12/12.6 to RyR was decreased in the hearts of hMR mice or WT mice treated with aldosterone compared with control WT (Figure 5B). Because RyR phosphorylation could influence the FKBP12/12.6-RyR association,[15,16] we examined RyR phosphorylation status after activation of the mineralocorticoid pathway. RyR contains multiple phosphorylation sites, including RyR-Ser2815 (phosphorylated by CaMKII)[27] and RyR-Ser2809 (phosphorylated by both CaMKII and PKA).[28] Using 2 different phosphospecific antibodies (RyR-PS2815 and RyR-PS2809) on SR fractions, we observed no difference in the ratio of phosphorylated RyR to total RyR among groups (Figure 5C). To distinguish FKBP12 versus FKBP12.6 expression, real-time quantitative polymerase chain reaction was used to assess mRNA levels with specific primers. At the mRNA level, decreased expression of both FKBP12 and FKBP12.6 was observed in the 3 models studied compared with respective controls (Figure 5D), whereas mRNA levels of RyR were not altered (data not shown).

Discussion

Long-term aldosterone exposure ex vivo or in vivo, or cardiac hMR expression in transgenic mice, increases the occurrence of DADs, in line with abnormal diastolic openings of RyR, which are associated with downregulation of FKBP12 and FKBP12.6. Although the link might be circumstantial, several lines of evidence suggest that overstimulation of the cardiac mineralocorticoid pathway may be a major upstream factor for aberrant Ca^{2+} release during diastole and may contribute to cardiac arrhythmia in HF.

Numerous experimental and clinical studies indicate that the aldosterone pathway participates in cardiac alterations associated with hypertension, HF, diabetes mellitus, and other pathologies.[1,3–6,12,14] Notably, inappropriate activation of cardiac MR is a likely participant in the development of poor outcomes for patients with HF, especially those associated with cardiac arrhythmia.[5,6] Interestingly, hMR mice showed high mortality and an increased occurrence of arrhythmia.[14] One of the possible cellular mechanisms for those arrhythmias is triggered activity caused by EADs and DADs, both of which are commonly associated with intracellular Ca^{2+} mishandling. We previously reported that along with AP lengthening, EADs occur in hMR mice.[14] The incidence of EADs was 1%, 11%, and 14% in ventricular myocytes isolated from WT, aldosterone-treated, and hMR littermate mice, respectively. In addition, we observed that 10% of rat ventricular myocytes incubated for 48 hours with aldosterone displayed EADs, whereas none were observed in control. Here, we found that the incidence of DAD was approximately 2-fold higher, thus constituting a substantial mechanism for aldosterone pathway–induced arrhythmias.

Although many Ca^{2+}-handling proteins are involved in DAD-related arrhythmias, abnormal opening of the RyR during diastole is an essential component.[7,8] We show here that the aldosterone pathway increased the occurrence and changed the spatiotemporal properties of spontaneous Ca^{2+} sparks. Similar alterations were found either ex vivo by incubation of adult cardiac myocytes with aldosterone or in

Figure 5 (Continued). to respective controls from WT (open bars), aldosterone-treated WT (WT+Aldo, hatched bar), and hMR (solid bars) mice and in rat ventricular myocytes incubated 48 hours with (+Aldo, solid bar) or without (cont, open bar) aldosterone 100 nmol/L. D, Real-time reverse-transcription polymerase chain reaction analysis of cardiac tissue content of FKBP12 and FKBP12.6. β_2-Microglobulin, GAPDH, HPRT, and UBC were used as reference genes, and relative mRNA levels were normalized to the geometric average of relative quantities for reference genes. *$P<0.05$.

Downloaded from http://circ.ahajournals.org/ at Cardiff University on February 19, 2014

vivo in mouse hearts, either after chronic delivery of aldosterone or after hMR expression. These consistent findings suggest that direct activation of cardiac MR by aldosterone modifies the Ca^{2+} spark phenotype, independent of other compensatory changes in vivo. Indeed, the ex vivo effects of aldosterone are prevented by a specific MR antagonist. In addition, hMR mice have increased aldosterone receptor activity, presumably due to physiological aldosterone levels, as assessed by prevention of phenotype effects with MR antagonist.[14] Moreover, MR antagonists also prevent other aldosterone-induced cardiac effects.[10,11,13]

Although we cannot exclude that the effects might be secondary to other modulations in myocyte Ca^{2+} handling, several lines of evidence suggest that activation of MR by aldosterone directly affects RyR activity. The increase in Ca^{2+} spark frequency is not due to an increase in SR Ca^{2+} load but rather might reflect a modulation of the intrinsic properties of the RyR complex. In addition to the increase in Ca^{2+} spark frequency, we observed a redistribution of Ca^{2+} sparks to long-lasting and broader populations. These "abnormal" Ca^{2+} sparks were also seen in control conditions but at a much lower frequency. Others have also found Ca^{2+} sparks that are longer or wider than the classic Ca^{2+} sparks in control conditions.[18,21,29–31] The incidence of wide (>2 μm) and long (60 to 80 ms) Ca^{2+} sparks is increased in left ventricular hypertrophy in the dog without alteration in Ca^{2+} spark amplitude.[32] Here, aldosterone exposure or cardiac hMR expression increased the proportions of long and wide Ca^{2+} sparks from a range of 4% to 6% to a range of 9% to 19% and from a range of 4% to 6% to a range of 16% to 30%, respectively, which constitutes a substantial effect. This indicates that aldosterone does not induce a new kind of Ca^{2+} spark but modifies the activity of functional release units.

Along with this alteration, we observed a significant downregulation of FKBP12 and FKBP12.6 expression without variation in the density of RyRs. Even if other alterations contributed to the observed modifications of Ca^{2+} spark characteristics, no other RyR-associated proteins have been shown to induce similar modulations to FKBP. FKBP12/12.6 binding to RyRs modulates the Ca^{2+}-flux properties of the channel complex; in particular, it regulates RyR open probability and stability at rest[20,33,34] (but see also Xiao et al[35]). FKBP12.6 removal by pharmacological approaches[22,36,37] or in transgenic animal models,[23] and conversely, adenoviral short-term FKBP12.6 overexpression,[21,38] modulated Ca^{2+} spark frequency and the occurrence of longer and wider Ca^{2+} sparks in a manner similar to that observed here. We showed that activation of the cardiac aldosterone pathway produced a decreased expression of FKBPs. In addition, we assessed the RyR-FKBP12/12.6 association in hMR transgenic and WT mice treated with aldosterone. The present results suggest that in mouse hearts, activation of the aldosterone pathway results in substantially reduced RyR-FKBP12/12.6 interaction, which could be the cause of the observed RyR-mediated Ca^{2+} leak. These effects are not associated with alteration of RyR phosphorylation status but might reflect a genomic regulation of FKBP12/12.6 by the cardiac aldosterone pathway, as evidenced by the decrease in mRNA levels of FKBP12 and FKBP12.6. Partial loss of FKBP12.6 from RyR in HF has been shown to cause diastolic Ca^{2+} leak, which may result in a greater tendency for DAD to occur and consequent triggered arrhythmias.[15,16,23,39–45] In addition, myocardial FKBP12.6 overexpression prevents triggered arrhythmias in normal hearts, probably by reducing diastolic SR Ca^{2+} leakage.[46] Beyond the controversial hypothesis that excess RyR activity due to hyperphosphorylation reduces RyR affinity for FKBP12.6,[47] most of the studies showed a reduction of FKBP protein level in HF.[23,39–45] Thus, we suggest that activation of the aldosterone pathway might be an essential step in the cascade of molecular events leading to FKBP deficiency that causes RyR Ca^{2+} leakage and triggers malignant cardiac arrhythmias in HF. Taken together, the present findings may explain in part why the use of MR antagonists in addition to optimal medical therapy is associated with improved survival and fewer sudden cardiac deaths in patients.

Sources of Funding

This work was supported by Agence Nationale de la Recherche (project No. A05071FS/APV05030FSA), Institut National de la Santé et de la Recherche Médicale (INSERM), the British Heart Foundation (PG/05/077), and the European Union (FPG, Life Science Genomics and Biotechnology for Health, #CT 2005 No. 018802, CONTICA).

Disclosures

None.

References

1. Williams JS, Williams GH. 50th Anniversary of aldosterone. *J Clin Endocrinol Metab*. 2003;88:2364–2372.
2. Arriza JL, Weinberger C, Cerelli G, Glaser TM, Handelin BL, Housman DE, Evans RM. Cloning of human mineralocorticoid receptor complementary DNA: structural and functional kinship with the glucocorticoid receptor. *Science*. 1987;237:268–275.
3. Weber KT. Aldosterone in congestive heart failure. *N Engl J Med*. 2001;345:1689–1697.
4. Rossi G, Boscaro M, Ronconi V, Funder JW. Aldosterone as a cardiovascular risk factor. *Trends Endocrinol Metab*. 2005;16:104–107.
5. Pitt B, Zannad F, Remme WJ, Cody R, Castaigne A, Perez A, Palensky J, Wittes J; Randomized Aldactone Evaluation Study Investigators. The effect of spironolactone on morbidity and mortality in patients with severe heart failure. *N Engl J Med*. 1999;341:709–717.
6. Pitt B, Remme W, Zannad F, Neaton J, Martinez F, Roniker B, Bittman R, Hurley S, Kleiman J, Gatlin M. Eplerenone, a selective aldosterone blocker, in patients with left ventricular dysfunction after myocardial infarction. *N Engl J Med*. 2003;348:1309–1321.
7. Bers DM. Cardiac excitation-contraction coupling. *Nature*. 2002;415:198–205.
8. Pogwizd SM, Bers DM. Cellular basis of triggered arrhythmias in heart failure. *Trends Cardiovasc Med*. 2004;14:61–66.
9. Clusin WT. Calcium and cardiac arrhythmias: DADs, EADs, and alternans. *Crit Rev Clin Lab Sci*. 2003;40:337–375.
10. Benitah JP, Vassort G. Aldosterone upregulates Ca^{2+} current in adult rat cardiomyocytes. *Circ Res*. 1999;85:1139–1145.
11. Benitah JP, Perrier E, Gomez AM, Vassort G. Effects of aldosterone on transient outward K^+ current density in rat ventricular myocytes. *J Physiol*. 2001;537:151–160.
12. Perrier E, Kerfant BG, Lalevee N, Bideaux P, Rossier MF, Richard S, Gomez AM, Benitah JP. Mineralocorticoid receptor antagonism prevents the electrical remodeling that precedes cellular hypertrophy after myocardial infarction. *Circulation*. 2004;110:776–783.
13. Perrier R, Richard S, Sainte-Marie Y, Rossier BC, Jaisser F, Hummler E, Benitah JP. A direct relationship between plasma aldosterone and cardiac L-type Ca^{2+} current. *J Physiol*. 2005;569:153–162.
14. Ouvrard-Pascaud A, Sainte-Marie Y, Benitah JP, Perrier R, Soukaseum C, Cat AN, Royer A, Le Quang K, Charpentier F, Demolombe S, Mechta-Grigoriou F, Beggah AT, Maison-Blanche P, Oblin ME, Delcayre C, Fishman GI, Farman N, Escoubet B, Jaisser F. Conditional mineralocorticoid receptor expression in the heart leads to life-threatening arrhythmias. *Circulation*. 2005;111:3025–3033.
15. Wehrens XH, Lehnart SE, Marks AR. Intracellular calcium release and cardiac disease. *Annu Rev Physiol*. 2005;67:69–98.

Downloaded from http://circ.ahajournals.org/ at Cardiff University on February 19, 2014

16. Yano M, Yamamoto T, Ikeda Y, Matsuzaki M. Mechanisms of disease: ryanodine receptor defects in heart failure and fatal arrhythmia. *Nat Clin Pract Cardiovasc Med*. 2006;3:43–52.
17. Nabhani T, Zhu X, Simeoni I, Sorrentino V, Valdivia HH, Garcia J. Imperatoxin A enhances Ca^{2+} release in developing skeletal muscle containing ryanodine receptor type 3. *Biophys J*. 2002;82:1319–1328.
18. Cheng H, Lederer WJ, Cannell MB. Calcium sparks: elementary events underlying excitation-contraction coupling in heart muscle. *Science*. 1993;262:740–744.
19. Bers DM. Macromolecular complexes regulating cardiac ryanodine receptor function. *J Mol Cell Cardiol*. 2004;37:417–429.
20. Fill M, Copello JA. Ryanodine receptor calcium release channels. *Physiol Rev*. 2002;82:893–922.
21. Gomez AM, Schuster I, Fauconnier J, Prestle J, Hasenfuss G, Richard S. FKBP12.6 overexpression decreases Ca^{2+} spark amplitude but enhances $[Ca^{2+}]_i$ transient in rat cardiac myocytes. *Am J Physiol Heart Circ Physiol*. 2004;287:H1987–H1993.
22. Xiao RP, Valdivia HH, Bogdanov K, Valdivia C, Lakatta EG, Cheng H. The immunophilin FK506-binding protein modulates Ca2+ release channel closure in rat heart. *J Physiol*. 1997;500(pt 2):343–354.
23. Xin HB, Senbonmatsu T, Cheng DS, Wang YX, Copello JA, Ji GJ, Collier ML, Deng KY, Jeyakumar LH, Magnuson MA, Inagami T, Kotlikoff MI, Fleischer S. Oestrogen protects FKBP12.6 null mice from cardiac hypertrophy. *Nature*. 2002;416:334–338.
24. Gaburjakova M, Gaburjakova J, Reiken S, Huang F, Marx SO, Rosemblit N, Marks AR. FKBP12 binding modulates ryanodine receptor channel gating. *J Biol Chem*. 2001;276:16931–16935.
25. George CH, Higgs GV, Lai FA. Ryanodine receptor mutations associated with stress-induced ventricular tachycardia mediate increased calcium release in stimulated cardiomyocytes. *Circ Res*. 2003;93:531–540.
26. Liu N, Colombi B, Memmi M, Zissimopoulos S, Rizzi N, Negri S, Imbriani M, Napolitano C, Lai FA, Priori SG. Arrhythmogenesis in catecholaminergic polymorphic ventricular tachycardia: insights from a RyR2 R4496C knock-in mouse model. *Circ Res*. 2006;99:292–298.
27. Wehrens XH, Lehnart SE, Reiken SR, Marks AR. Ca^{2+}/calmodulin-dependent protein kinase II phosphorylation regulates the cardiac ryanodine receptor. *Circ Res*. 2004;94:e61–e70.
28. Marx SO, Reiken S, Hisamatsu Y, Jayaraman T, Burkhoff D, Rosemblit N, Marks AR. PKA phosphorylation dissociates FKBP12.6 from the calcium release channel (ryanodine receptor): defective regulation in failing hearts. *Cell*. 2000;101:365–376.
29. Parker I, Wier WG. Variability in frequency and characteristics of Ca^{2+} sparks at different release sites in rat ventricular myocytes. *J Physiol*. 1997;505(pt 2):337–344.
30. Blatter LA, Huser J, Rios E. Sarcoplasmic reticulum Ca^{2+} release flux underlying Ca^{2+} sparks in cardiac muscle. *Proc Natl Acad Sci U S A*. 1997;94:4176–4181.
31. Shirokova N, Gonzalez A, Kirsch WG, Rios E, Pizarro G, Stern MD, Cheng H. Calcium sparks: release packets of uncertain origin and fundamental role. *J Gen Physiol*. 1999;113:377–384.
32. Song LS, Pi Y, Kim SJ, Yatani A, Guatimosim S, Kudej RK, Zhang Q, Cheng H, Hittinger L, Ghaleb B, Vatner DE, Lederer WJ, Vatner SF. Paradoxical cellular Ca^{2+} signaling in severe but compensated canine left ventricular hypertrophy. *Circ Res*. 2005;97:457–464.
33. Lehnart SE, Huang F, Marx SO, Marks AR. Immunophilins and coupled gating of ryanodine receptors. *Curr Top Med Chem*. 2003;3:1383–1391.
34. Chelu MG, Danila CI, Gilman CP, Hamilton SL. Regulation of ryanodine receptors by FK506 binding proteins. *Trends Cardiovasc Med*. 2004;14:227–234.
35. Xiao J, Tian X, Jones PP, Bolstad J, Kong H, Wang R, Zhang L, Duff HJ, Gillis AM, Fleischer S, Kotlikoff M, Copello JA, Chen SR. Removal of FKBP12.6 does not alter the conductance and activation of the cardiac ryanodine receptor or the susceptibility to stress-induced ventricular arrhythmias. *J Biol Chem*. 2007;282:34828–34838.
36. McCall E, Li L, Satoh H, Shannon TR, Blatter LA, Bers DM. Effects of FK-506 on contraction and Ca^{2+} transients in rat cardiac myocytes. *Circ Res*. 1996;79:1110–1121.
37. Yoshihara S, Satoh H, Saotome M, Katoh H, Terada H, Watanabe H, Hayashi H. Modification of sarcoplasmic reticulum (SR) Ca2+ release by FK506 induces defective excitation-contraction coupling only when SR Ca2+ recycling is disturbed. *Can J Physiol Pharmacol*. 2005;83:357–366.
38. Loughrey CM, Seidler T, Miller SL, Prestle J, MacEachern KE, Reynolds DF, Hasenfuss G, Smith GL. Over-expression of FK506-binding protein FKBP12.6 alters excitation-contraction coupling in adult rabbit cardiomyocytes. *J Physiol*. 2004;556:919–934.
39. Shou W, Aghdasi B, Armstrong DL, Guo Q, Bao S, Charng MJ, Mathews LM, Schneider MD, Hamilton SL, Matzuk MM. Cardiac defects and altered ryanodine receptor function in mice lacking FKBP12. *Nature*. 1998;391:489–492.
40. Yano M, Ono K, Ohkusa T, Suetsugu M, Kohno M, Hisaoka T, Kobayashi S, Hisamatsu Y, Yamamoto T, Noguchi N, Takasawa S, Okamoto H, Matsuzaki M. Altered stoichiometry of FKBP12.6 versus ryanodine receptor as a cause of abnormal Ca^{2+} leak through ryanodine receptor in heart failure. *Circulation*. 2000;102:2131–2136.
41. Reiken S, Gaburjakova M, Gaburjakova J, He K-l, Prieto A, Becker E, Yi G, Wang J, Burkhoff D, Marks AR. β-Adrenergic receptor blockers restore cardiac calcium release channel (ryanodine receptor) structure and function in heart failure. *Circulation*. 2001;104:2843–2848.
42. Wehrens XH, Lehnart SE, Reiken SR, Deng SX, Vest JA, Cervantes D, Coromilas J, Landry DW, Marks AR. Protection from cardiac arrhythmia through ryanodine receptor-stabilizing protein calstabin2. *Science*. 2004;304:292–296.
43. Yano M, Okuda S, Oda T, Tokuhisa T, Tateishi H, Mochizuki M, Noma T, Doi M, Kobayashi S, Yamamoto T, Ikeda Y, Ohkusa T, Ikemoto N, Matsuzaki M. Correction of defective interdomain interaction within ryanodine receptor by antioxidant is a new therapeutic strategy against heart failure. *Circulation*. 2005;112:3633–3643.
44. Ai X, Curran JW, Shannon TR, Bers DM, Pogwizd SM. Ca^{2+}/calmodulin-dependent protein kinase modulates cardiac ryanodine receptor phosphorylation and sarcoplasmic reticulum Ca^{2+} leak in heart failure. *Circ Res*. 2005;97:1314–1322.
45. Huang F, Shan J, Reiken S, Wehrens XH, Marks AR. Analysis of calstabin2 (FKBP12.6)-ryanodine receptor interactions: rescue of heart failure by calstabin2 in mice. *Proc Natl Acad Sci U S A*. 2006;103:3456–3461.
46. Gellen B, Fernandez-Velasco M, Briec F, Vinet L, LeQuang K, Rouet-Benzineb P, Benitah JP, Pezet M, Palais G, Pellegrin N, Zhang A, Perrier R, Escoubet B, Marniquet X, Richard S, Jaisser F, Gomez AM, Charpentier F, Mercadier JJ. Conditional FKBP12.6 overexpression in mouse cardiac myocytes prevents triggered ventricular tachycardia through specific alterations in excitation-contraction coupling. *Circulation*. 2008;117:1778–1786.
47. Bers DM, Eisner DA, Valdivia HH. Sarcoplasmic reticulum Ca^{2+} and heart failure: roles of diastolic leak and Ca^{2+} transport. *Circ Res*. 2003;93:487–490.

CLINICAL PERSPECTIVE

Defective calcium handling is a key contributor to the pathophysiology of heart failure, not only in the weakening of the heart's ability to pump blood but also in the erratic heart beats that cause sudden death. Research conducted to understand the molecular mechanisms underlying those fatal arrhythmias has focused mainly on downstream mechanisms (the defective calcium-handling processes) rather than the causes. The present study highlights the role of the cardiac aldosterone pathway as an upstream primary molecular event that leads to defective calcium handling. Combining ex vivo and in vivo (transgenic mice) approaches and using state-of-the-art Ca^{2+} imaging, electrophysiology, and biochemistry methods, we provide the first evidence that downregulation of FK506 binding proteins (also known as calstabins) through the aldosterone pathway causes defectiveness of ryanodine receptor activity, which has been associated with the common pathogenic mechanism of sudden cardiac death and heart failure. In addition, these findings underline the potential of mineralocorticoid receptor antagonists as antiarrhythmic therapy.

Downloaded from http://circ.ahajournals.org/ at Cardiff University on February 19, 2014

SUPPLEMENTAL METHODS

FK506 binding protein level in cell lysates.

Cell lysate protein (75 μg) was fractionated on 20 % SDS-PAGE gels, transferred onto nitrocellulose membranes (1 h at 100 V, 0.45 μm Hybond ECL, GE Healthcare Bio-Sciences Corp, NJ, USA) and probed with anti-FKBP12/12.6 serum (Santa Cruz Biotechnology) diluted 1:200 in PBST buffer (in mmol/L: KH_2PO_4 3, Na_2HPO_4 10, NaCl 150, 0.1% Tween 20, pH 7.2-7.4) with 1 % bovine serum albumin (BSA). Membranes were blocked overnight with 3 % BSA in PBST buffer before primary antibody addition. Membranes were incubated 2 hour with secondary peroxidase-conjugate goat antiserum (diluted 1:15,000 in PBST, Sigma). Signals were developed by chemiluminiscence (Supersignal West Pico Chemiluminescent substrate, Pierce Biotechnology). The relative amount of protein on the blots was determined by densitometry using KodakID Software (v. 3.635, Molecular Imaging Systems). Actin signals were detected in the same blots with anti-actin serum (Sigma) and used as loading controls.

RyR-FKBP12/12.6 association on SR fractions.

SR fractions (50 μg) were resuspended in SDS-PAGE loading buffer (60 mmol/L Tris, 2% SDS, 10% glycerol, 5mmol/L EDTA, 2% β-mercaptoethanol, 0.01% bromophenol blue, pH 6.8), heated at 85°C for 5min, and proteins were separated in a 4% SDS-PAGE gel strengthened with 0.5% agarose (for RyR analysis), or a 15% SDS-PAGE gel (for FKBP analysis). Proteins from 4% gels were electrophoretically transferred to a polyvinylidene difluoride membrane (Immobilon-P, Millipore) using a semi-dry transfer system (Trans-Blot SD, Bio-Rad) in transfer buffer (48mmol/L Tris, 39mmol/L glycine, 0.0375% SDS) at 22V for 4 hours. Proteins from 15% gels were transferred to PVDF membrane using a mini-wet blot transfer system (Bio-Rad) in buffer (26mmol/L Tris, 192mmol/L glycine, 20% methanol) at 200 mA for 1 hour. Primary antibodies were applied overnight at 4°C: FKBP12/12.6

antibody at 1:200 dilution (Affinity BioReagents), RyR antibody at 1:1000 dilution (rabbit polyclonal antibody raised to RyR residues 4454-4474). Immunoreactive protein bands were visualized by enhanced chemiluminescence detection (ECL, GE Healthcare). Densitometric analysis was performed using a GS-700 scanner (Bio-Rad) and Quantity One software (Bio-Rad).

RyR phosphorylation.

75 µg of protein were fractionated on 7.5 % SDS-PAGE gels, transferred onto PVDF membranes (2 h at 100 V, 0.45 µm Amersham). Then membranes were probed successively (after successive membrane stripping in 1mol/L Glycine solution [pH 7.2]) with anti-RyR (C3–33, 1:3000 diluted in PBST solution, Affinity BioReagents), anti–RyR-PS2809 (1:5000, Badrilla) and anti–RyR-PS2815 (1:5000) antibodies generously provided by Dr A.R. Marks (Columbia University, New York) diluted in TBST solution (in mmol/L Tris-HCl 50, NaCl 150, 0.1% Tween 20, pH 7.4). Antibodies were revealed with secondary peroxidase-conjugate mouse or rabbit antiserum (1:15,000, Calbiochem).

Ca^{2+} sparks analysis.

Ca^{2+} sparks were recorded in intact myocytes loaded with fluorescent Ca^{2+} dye (Fluo-3 AM) Spontaneous Ca^{2+} sparks were obtained in quiescent cells. SR Ca^{2+} load was estimated by rapid caffeine (10 mmol/L) application. Images were obtained with a confocal microscopy (Meta Zeiss LSM 510, objective w.i. 63x, n.a. 1.2) by scanning the cell with an Argon laser every 1.54 ms; fluorescence was excited at 488 nm and emissions were collected at >505 nm. Image analyses were performed by homemade routines using IDL software (Research System Inc.). Images were corrected for the background fluorescence. The fluorescence values (F) were normalized by the basal fluorescence (F_0) in order to obtain the fluorescence ratio (F/F_0).

The probability density functions $PDf(a) = \frac{N(a)}{N_{total} \cdot \Delta}$, where N(a) is the histogram distribution of Ca^{2+} spark parameter a, N_{total} is the total number of Ca^{2+} sparks and Δ is the binwidth, were modelled as a mixture of Gauss distributions according to:

$$\sum_{i=1}^{i} \frac{p_i}{\sqrt{2\Pi} \cdot \sigma_i} e^{-\frac{1}{2}\left(\frac{x-\mu_i}{\sigma i}\right)^2} \text{ and } \sum_{i=1}^{i} p_i = 1$$

where P_i is the proportion, μ_i the mean and σ_i the standard deviation of individual distribution.

Goodness of fits were always examined by χ^2 test (Σ (observed-expected)^2/expected) and in all the cases >0.05, indication of the absence of major discrepancy between distributions and fits.

For Ca^{2+} spark duration, analysis was conducted on log-transformed FDHM and the results are presented after back transformation, using the delta method $(\sigma_I * 10^{mean^2})^{1/2}$ for conversion of σ_i.

SUPPLEMENTAL TABLES

Table S1. Primers used in real-time RT-PCR assays

Gene	Oligonucleotide sequence	
	Mice	Rat
FKBP12	F-5'-ACTAGGCAAGCAGGAGGTGA-3'	F-5'-ACTAGGCAAGCAGGAGGTGA-3'
	R-5'-CTCCATAGGCATAGTCTGAGGAGAT-3'	R-5'-CATAGGCATAGTCTGGGGAGAT-3'
FKBP12.6	F-5'-AGAAGGCACTGCCCAGATGA-3'	F-5'-AGAAGGCGCTGCCCAGATGA-3'
	R-5'-AAAGATGAGGGTGGCATTGG-3'	R-5'-AAAGATGAGGGTGGCATTGG-3'
RyR	F-5'-CTTCGATGTTGGCCTTCAAGAG-3'	F-5'-GATGTTGGCCTTCAAGAGGATACCACA-3'
	R-5'-CCAACACGCACTTTTTCTCCTT-3'	R-5'-CCAACCCGCACCTTTTCTCCTT-3'
β_2-μG	F-5'-TTCTATATCCTGGCTCACACTGAA-3'	F-5'-TTCTACATCCTGGCTCACACTGAA-3'
	R-5'-CACATGTCTCGATCCCAGTAGA-3'	R-5'-ACATGTCTCGGTCCCAGGTGA-3'
GAPDH	F-5'-AATGGTGAAGGTCGGTGTG-3'	F-5'-TGATTCTACCCACGGCAAGTT-3'
	R-5'-GAAGATGGTGATGGGCTTCC-3'	R-5'-TGATGGGTTTCCCATTGATGA-3'
HPRT	F-5'-CTCAACTTTAACTGGAAAGAATGTC-3'	F-5'-CTCAACTTTAACTGGAAAGAATGTC-3'
	R-5'-TCCTTTTCACCAGCAAGCT-3'	R-5'-TCCTTTTCACCAGCAAGCT-3'
UBC	F-5'-AGCCCAGTGTTACCACCAAG-3'	F-5'-AGCCCAGTGTTAACACCAAG-3'
	R-5'-ACCCAAGAACAAGCACAAGG-3'	R-5'-ACCCAAGAACAAGCACAAGG-3

F and R, foward and reverse primers, respectively. Reference genes: β_2-μG, β_2-microglobulin, GAPDH, Glyceraldehyde 3-phosphate dehydrogenase, HPRT, Hypoxanthine-guanine phosphoribosyltransferase, UBC, ubiquitin C.

Table S2. Parameter estimates from mixed-effect models with random effects for animals and cells.

	Ca^{2+} spark frequency ($s^{-1}.100\mu m^{-1}$)		
	Least Squares Mean	95% confidence interval	*P*-value *vs.* respective control
Aldo *in vivo*			
WT	1.03	0.86 to 1.23	
WT+Aldo	1.82	1.51 to 2.21	0.023
hMR	1.79	1.49 to 2.14	0.023
Global Type 3 test		*P*=0.0347	
Aldo *ex vivo*			
control	0.70	0.55 to 0.89	
Aldo	1.50	1.17 to 1.92	0.0052
Aldo+RU	0.61	0.46 to 0.80	0.4880
Global Type 3 test		*P*=0.0056	
	Ca^{2+} spark full width at half maximal amplitude (μm)		
Aldo *in vivo*			
WT	2.68	2.60 to 2.77	
WT+Aldo	2.79	2.71 to 2.88	0.0346
hMR	3.02	2.93 to 3.10	0.0119
Global Type 3 test		*P*=0.0253	
Aldo *ex vivo*			
control	2.55	2.44 to 2.66	
Aldo	2.88	2.77 to 2.99	0.0069
Aldo+RU	2.53	2.40 to 2.66	0.8183
Global Type 3 test		*P*=0.0091	
	Ca^{2+} spark full duration at half maximal amplitude (ms)		
Aldo *in vivo*			
WT	31.62	28.48 to 35.11	
WT+Aldo	33.25	29.93 to 36.95	0.0553
hMR	39.02	35.20 to 43.24	0.0337
Global Type 3 test		*P*=0.0655	
Aldo *ex vivo*			
control	37.12	33.60 to 41.01	
Aldo	43.98	40.03 to 48.31	0.0515
Aldo+RU	34.20	30.57 to 38.26	0.3259
Global Type 3 test		*P*=0.0345	